

## **Brain BOLD MRI O<sub>2</sub> and CO<sub>2</sub> stress testing: Implications for perioperative neurocognitive disorder following surgery**

W. Alan C. Mutch, MD, FRCPC<sup>1,5\*</sup>, Renée El-Gabalawy, PhD<sup>1,2</sup>, Lawrence Ryner, PhD<sup>3,4,5</sup>, Josep Puig, MD, PhD<sup>3</sup>, Marco Essig, MD<sup>3,5</sup>, Kayla Kilborn<sup>1</sup>, Kelsi Fidler<sup>1</sup>, M. Ruth Graham, MD, FRCPC<sup>1,5</sup>

**Departments:** Anesthesiology, Perioperative and Pain Medicine<sup>1</sup>, Clinical Health Psychology<sup>2</sup>, Radiology<sup>3</sup>, Physics<sup>4</sup> University of Manitoba; Canada North Concussion Network ([www.CNCN.ca](http://www.CNCN.ca))<sup>5</sup>

**Short Title:** Brain BOLD imaging with supplemental O<sub>2</sub> and CO<sub>2</sub>

**Key Words:** anaesthesia, CO<sub>2</sub>, O<sub>2</sub>, BOLD, MRI, surgery, delirium, cognitive dysfunction

**\*Corresponding Author:** WACM

**Mailing address:** Department of Anesthesiology, Perioperative and Pain Medicine  
2nd Floor, Harry Medovy House, 671 William Ave. Max Rady College of Medicine, University of Manitoba, Winnipeg, MB R3E 0Z2 Canada

**Phone:** 204-787-1414

**Fax:** 204-787-4291

**Text body word count:** 3380

**Abstract word count:** 177

**Funding:** Manitoba Health Research Fund (wacm); Anesthesia Oversight Committee Fund (wacm, rel-g, mrg); Manitoba Public Insurance Corporation (me, wacm)

**Conflict of interest:** None declared

## **Abstract:**

Respiratory end-tidal (ET) gas control is fundamental to anaesthetic management. The range of ET O<sub>2</sub> and CO<sub>2</sub> during the conduct of anaesthesia can significantly deviate from values in the awake state. Recent work shows ET CO<sub>2</sub> influences the incidence of perioperative neurocognitive disorder (POND). We examine the effects of controlled alterations in both ET O<sub>2</sub> and CO<sub>2</sub> on cerebral blood flow (CBF) in awake adults using BOLD MRI. Twelve healthy adults had BOLD and CBF responses measured to alterations in ET CO<sub>2</sub> and O<sub>2</sub> in various combinations commonly observed under anaesthesia. Dynamic alterations in regional BOLD and CBF were seen in all subjects with expected and inverse responses to both stimuli. These effects were incremental and rapid (within seconds). The most dramatic effects were seen with combined hyperoxia and hypocapnia. Inverse responses increased with age. Here we show that human brain CBF responds dramatically to alterations in ET respiratory gas tensions commonly seen during anaesthesia. Such alterations may impact the observed incidence of POND following surgery and intensive care, and is an important area for further investigation.

Perioperative neurocognitive disorder (POND) is a newly proposed nomenclature to classify cognitive problems that can manifest after anaesthesia and surgery.<sup>1</sup> The term encompasses pre-existing problems such as mild cognitive impairment or dementia, acute postoperative delirium, and postoperative cognitive dysfunction, with the potential for learning and memory deficits in young children and a progressive downward arc in cognitive abilities in older adults after surgery. Despite efforts to apply consistent terminology to facilitate research in this area, the phenomenon of POND continues to be poorly understood. The cost to society of this problem is immense and new insights are desperately needed.<sup>234</sup> Putative causative factors include, first, the potential neurotoxicity of the anaesthetic agents themselves<sup>5678</sup>. The basic premise is that the neurotransmitter modulating effects of anaesthetic agents damage neurons or their dendrites at the extremes of life and lead to caspase induced apoptosis.<sup>910</sup> Evidence supporting this is unequivocal in animal models up to and including non-human primates.<sup>1112</sup> However, translation to the human domain is contradictory and an increasing series of clinical studies, both in children and adults have failed to provide the expected surrogates for evidence of neuronal damage as seen in animal models of anaesthetic neurotoxicity. Many of the animal models are highly constrained by specific requirements to demonstrate neuronal injury. An overview of some of these translational issues has been recently highlighted.<sup>131415</sup> The large retrospective studies that have failed to show an association between anaesthetic exposure or multiple exposures and neurocognitive deficits may be criticized as not being fine grained enough to address the problem. However, more recent prospective trials also fail to show a signal of POND either in children or adults. For example, a paediatric study failed to show any difference in the primary outcome of individual intelligence quotient testing later in childhood when anaesthesia naive children were compared to propensity matched children undergoing surgery at less than 3 years of age with either single or multiple anaesthetic exposure.<sup>16</sup> An adult study failed to show a decrease in postoperative delirium in older adults with anaesthetic depth minimized by limiting EEG burst suppression compared to those managed conventionally with a greater depth of anaesthesia.<sup>17</sup> In light of these null findings, new insights appear warranted.

Alternative considerations include neuroinflammatory effects consequent with surgical stress<sup>181920</sup>, and premorbid risk factors (e.g., cognitive dysfunction, psychiatric illness, increasing age) which may influence the incidence of POND.<sup>32122</sup> More recent work suggests that a multi-factorial approach, described as a stress-diathesis model<sup>23</sup>, may provide further insights. In this model, the conduct of anaesthesia, which includes the management of respiratory gases during mechanical ventilation, may contribute to the stress of the perioperative period in vulnerable individuals (the diathesis) and is associated with development of POND.<sup>23</sup>

Although respiratory end-tidal gas control is a fundamental principle of anaesthetic management, the range of end-tidal (ET) O<sub>2</sub> and CO<sub>2</sub> typically seen during the conduct of anaesthesia can significantly deviate from the awake baseline state, but has not been considered as a potential contributor to POND in previous investigations. Periods of both hypocapnia during mechanical ventilation and hypercapnia during the reestablishment of spontaneous ventilation are common. The use of 100% oxygen during anaesthesia induction and emergence and maintenance of anaesthesia with O<sub>2</sub> concentrations of 50% are typical.

The effects of these alterations in respiratory gases have significant effects on cerebral blood flow and oxygenation which may be implicated in cognitive dysfunction. In the present study, using blood oxygenation level dependent (BOLD) and pseudo continuous arterial spin labeling (pCASL) MRI, we examine the effects of controlled alterations in ET O<sub>2</sub> and CO<sub>2</sub> in various combinations commonly observed during anaesthesia and surgery on cerebral blood flow (CBF) in 12 healthy awake adults. Based on the significant alterations in CBF observed, we propose mechanisms to suggest that manipulation of the gases of respiration (O<sub>2</sub> and CO<sub>2</sub>) may be a significant contributor to the intraoperative stress leading to POND in vulnerable individuals.<sup>2425</sup> The proposed mechanisms described here can be easily examined and ruled in or out based on well-conducted clinical trials.

### **Methods:**

These studies relate to ongoing examination of volunteer subjects and patients undergoing surgical intervention and concussion studies at the University of Manitoba (U of M), Winnipeg, Canada. The protocol was approved by the Biomedical Research Ethics Board (BREB), at the U of M, and a cohort of the study group was registered at ClinicalTrials.gov for some components of the study NCT02126215. For the present study, 12 healthy adult volunteers gave witnessed informed consent and underwent MRI while ET gases were manipulated in a controlled fashion with a RespirAct (a computer-controlled model-based prospective end-tidal gas mixer).<sup>2627</sup> The volunteers had no neurological health issues nor were receiving psychotropic drugs for any psychiatric conditions. None had a history of POND with any previous surgery.

*End-tidal gas protocols* – Following a brief overview, subjects had an air-tight plastic mask affixed to their face. They then were positioned on the imaging table and a prep sequence was run on the RespirAct to determine the individual's resting ET gases, breathing frequency and tidal volume. When determined, the subject was positioned in the magnet bore. Breathing sequences (see Supplemental File 1 for an example) included i) a CO<sub>2</sub> ramp protocol; an 11-minute sequence of baseline ET CO<sub>2</sub> (1-min), a square wave increase in ET CO<sub>2</sub> by 5 mm Hg (1-min), a return to baseline (1-min), a square wave period of spontaneous hyperventilation upon command to decrease ET CO<sub>2</sub> by 5 mm Hg (1-min), a 6-min ramp increase in CO<sub>2</sub> to 10 mm Hg above baseline, a 1-min return to baseline CO<sub>2</sub>. During this sequence the ET O<sub>2</sub> was clamped at 100 mm Hg; ii) an O<sub>2</sub> ramp protocol; an 11-minute sequence of baseline ET O<sub>2</sub> fixed at 100 mm Hg (1-min), a square wave increase in ET O<sub>2</sub> to 500 mm Hg (1-min, 400 mm Hg above baseline), a return to baseline (2-min), a 6-min ramp increase in O<sub>2</sub> to 400 mm Hg above baseline, a 1-min return to baseline O<sub>2</sub>. During this sequence the ET CO<sub>2</sub> was clamped at the subject's baseline determined from the initial CO<sub>2</sub> ramp sequence; iii) pCASL sequence 1 (a 3-min baseline sequence and a block design square wave alteration); baseline O<sub>2</sub> for 3-min, then square wave increase in O<sub>2</sub> to 400 mm Hg (hyperoxia) with ET CO<sub>2</sub> clamped at subject baseline (normocapnia); iv) pCASL sequence 2, after a 5-minute re-equilibration period; baseline CO<sub>2</sub> for 3-min, then square wave increase in CO<sub>2</sub> to 5 mm Hg above baseline (hypercapnia), with ET O<sub>2</sub> clamped at 100 mm Hg (normoxia); pCASL sequence 3, after a 5-minute re-equilibration period; baseline CO<sub>2</sub> and ET O<sub>2</sub> at 100 mm Hg for 3-min, then square wave decrease in CO<sub>2</sub> by 5 mm Hg below baseline

(hypocapnia) by spontaneous hyperventilation on command and ET O<sub>2</sub> increased to 400 mm Hg (hyperoxia).

*Imaging protocols* – Imaging occurred on a Siemens 3T Verio magnet. The head coil had 12-channels. Each subject underwent gradient field mapping, magnetization-prepared rapid acquisition with gradient echo (MPRAGE) anatomic imaging, gradient recalled echo (GRE) BOLD imaging × 2 for the ramp protocols, an M0 calibration image for each of the pCASL sequences, pCASL × 3 for cerebral blood flow determination during the various end-tidal gas protocols, axial fluid attenuated inversion recovery (AX-FLAIR) and AX-T2\* GRE. The BOLD GRE images were obtained using Siemens proprietary software for prospective motion correction (PACE). See Supplemental File 2 for a fuller description of the imaging sequences. Total imaging time was approximately 45-60 minutes/session.

*Post-processing of images* – The images were converted to .nii files and using custom written batch files preprocessing was accomplished using standard SPM8 pipelines. BOLD images were re-aligned, co-registered to the MPRAGE images, normalized and smoothed with a 5×5×5 mm smoothing kernel at FWHM. These images were then fit to a GLM based on the end-tidal CO<sub>2</sub> and O<sub>2</sub> ramps respectively. Both the expected and the inverse responses were examined at various p-values. First and 2<sup>nd</sup> level analysis were undertaken for the images; the 2<sup>nd</sup> level using a leave-one-out approach. Various masks were applied to the images to examine specific regions and control for excessive alteration in B0 field strength. See Supplemental File 3 for a description of the masks used. The pCASL images were processed using the ASLtbx developed by Ze Wang.<sup>28</sup> Cerebral blood flow as determined at the baseline settings for each of the three runs and the altered CBF determined for cerebrovascular reactivity (CVR) assessment of the block-designed change in flow. Flow maps were determined for baseline settings, the block-designed stress and the difference between.

## Results:

Twelve studies were undertaken. In all, CO<sub>2</sub> and O<sub>2</sub> BOLD GRE ramp protocols were undertaken and completed. In 6, pCASL measurements were obtained. In these, the first two pCASL protocols were completed in all cases and all 3 pCASL protocols were completed in 4 subjects. There were no complications noted following completion of the protocols.

Subject demographics are seen in Table 1. One subject had a history of migraine headaches and one subject had a prior history (remote) of concussion.

The end-tidal gas results are shown in Table 2. All subjects had ET gas control close to their planned alterations. A plateau was seen for the upper limit of ET O<sub>2</sub> for all with a maximum in the range of 475 mm Hg in the O<sub>2</sub> ramp protocol. The 1<sup>st</sup> level analysis from the SPM processing fit to the general linear model (GLM) for the CO<sub>2</sub> ramp is shown in Table 3. The raw voxel counts are with an individualised grey and white matter inclusive mask only and the masked voxel counts are following application of the individualised mask as shown in Supplemental File 3. The 1<sup>st</sup> level analysis from the SPM processing fit to the general linear model (GLM) for the O<sub>2</sub> ramp is shown in Table 4. Table 5 and 6 show the 2<sup>nd</sup> level analysis

for CO<sub>2</sub> and O<sub>2</sub> ramps respectively. A group comparison of the 4 individuals with masked voxels counts greater than 50 for inverse responses to the CO<sub>2</sub> and O<sub>2</sub> ramps is shown in Supplemental File 4. An example of 1 subject for the brain BOLD and inverse response to the CO<sub>2</sub> ramp at clamped O<sub>2</sub> is shown in Figure 1 and the BOLD response in the same patient to the O<sub>2</sub> ramp at clamped CO<sub>2</sub> is shown in Figure 2. There is an association with increasing inverse voxel counts response to CO<sub>2</sub> and O<sub>2</sub> with increasing age. This correlation best fit a 2<sup>nd</sup> order polynomial;  $r = 0.664$ ,  $p = 0.019$  (Figure 3). A result from the 2<sup>nd</sup> level analysis is also shown. An individual response to the pCASL protocol is shown in Figure 4. For this subject the pCASL CVR responses are shown for hypercapnia at isoxia (A), hyperoxia at isocapnia (B) and hyperoxia with hypocapnia (C). With hypocapnia the decrement in CBF becomes marked. The heterogeneity of BOLD to CBF response to the O<sub>2</sub> ramp and hyperoxia-baseline CVR response is shown in Figure 5. The decrease in CBF with decreased BOLD signal is highlighted for the frontal cortex. The inverse response to hyperoxia is associated with a regional decrement in CBF. The dynamism of responsiveness to alterations in respiratory gases is evident.

### **Discussion:**

The results of this study provide preliminary evidence of the detrimental impact of respiratory gas stress on the human brain, and have important implications for the conduct of anaesthesia on POND. This imaging study was undertaken to develop an atlas of healthy adults for comparison purposes for research protocols examining cerebrovascular reactivity (CVR) to CO<sub>2</sub> and O<sub>2</sub> in a number of disease states. Prior work by a number of members of this group, have used similar approaches to study concussion in adolescent patients.<sup>293031</sup> As these CVR studies evolved it became apparent that the findings may have considerable import regarding the conduct of anaesthesia and control of ET respiratory gases with the potential to influence the incidence and severity of perioperative neurocognitive disorder (POND). Reinforcing this is the finding that intraoperative hypocapnia is associated with an increased incidence of POND<sup>2332</sup> in adults greater than 60 years undergoing major non-cardiac surgery. Also reconfirmed is a signal indicating greater inverse CO<sub>2</sub> responsiveness in older subjects (discussed in Supplemental File 4). This signal has previously been identified as a biomarker for POND in these patients after surgery.<sup>23</sup> As such, examination of the potential consequences of alterations in CVR to respiratory gases during anaesthesia and surgery appears warranted.

Anaesthetic management comprises more than just administration of controlled doses of either volatile or intravenous agents to render the patient insensate. Intraoperative management also includes haemodynamic control and breath-to-breath management and monitoring of respiratory gases – O<sub>2</sub> and CO<sub>2</sub>. Oxygen is usually given in increased fractional concentrations over that seen in room air ( $FiO_2 = 0.21$ ). It is not uncommon to administer a significantly elevated O<sub>2</sub> (such as an  $FiO_2 = 0.50$ ) for the duration of a surgical case and  $FiO_2 = 1.0$  is virtually always given at the start and end of surgical cases as a buffer for the risk of hypoxia. Except for short surgical procedures, patients are usually mechanically ventilated which is frequently associated with lower tensions of ET CO<sub>2</sub> for the duration of the

intraoperative procedure.<sup>3334</sup> High tensions of CO<sub>2</sub> are also not uncommon at the end of a procedure with reversal of muscle relaxants and reestablishment of spontaneous ventilation. Thus, even during a routine anaesthetic, respiratory gases usually have a wide range of fluctuation (far outside the range seen in the awake healthy state). The potential for large variation in CBF with such alterations in ET gases during conduct of even a normal anaesthetic can be deduced by examination of the various images from this study. A marked dynamism is clear and in certain subjects 'steal' phenomena are seen where the inverse response to expected changes in BOLD signal or CBF to CO<sub>2</sub> alterations and O<sub>2</sub> are evident. This is especially pronounced in the frontal cortex where executive function resides, potentially placing this critical area of the brain at risk with alterations in respiratory gases during anaesthesia.

Mechanistically the inverse responses to changing ET tensions of CO<sub>2</sub> and O<sub>2</sub> differ. The 'intracranial steal' seen with hypercapnia is well elucidated.<sup>35</sup> Regional areas of vasoparalysis result in shunting of blood from their perfused areas to adjacent regions with increasing adjacent regional vasodilation with hypercapnia. The regional 'intracranial steal' seen with hyperoxia appears the reverse. Excessive regional vasoconstriction seems evident. Surrounding areas with less vasoconstriction receive higher flow. The inverse BOLD response suggests vasoconstriction of such intensity that venular offloading of oxygen from hemoglobin is excessive here, resulting in increased paramagnetic signal.<sup>3637</sup> This explanation suggests excessive regional vascular tone in these feeding vessels – the mechanism to be further elucidated. It has been noted however, that frontal neurons in Alzheimer transgenic mice are vulnerable to hyperoxia through synaptic dysfunction and brain oxidative stress.<sup>38</sup> Vasoconstriction with hyperoxia is a proposed mechanism in this model.<sup>3940</sup> Examination of the inverse BOLD responses seen in the BOLD signal curve fits in Figure 1 and 2 indicates that both the response to CO<sub>2</sub> and O<sub>2</sub> alterations are rapid and incremental, indicating a very dynamic process. The pCASL findings indicate that the regional vasoconstrictive influence of hyperoxia is amplified in the presence of hypocapnia (Figure 4). As noted above, this combination of ET gas conditions is ubiquitous during the conduct of anaesthesia. The curve fit examining the magnitude of inverse voxels fits a second order polynomial correlated to increasing age although the sample size is small. The best fit to a paraboloid, however, is an interesting finding as the incidence of POND is bimodal at the extremes of life. Whether inverse voxel signatures are more evident in neonates and young children is an open question.

These control studies have been conducted in awake individuals so the impact of anaesthesia – both from volatile agents (known cerebral vasodilators) and intravenous agents (know cerebral vasoconstrictors with the exception of ketamine) may alter the response to CO<sub>2</sub> and O<sub>2</sub> as seen here. However, a carefully done study in rats anaesthetized with isofluane (a volatile agent) reports many of the same BOLD and CBF findings using similar imaging approaches, suggesting that the respiratory gas effects on cerebral perfusion translate to the anaesthetized state with volatile agents.<sup>41</sup> Recent work by Venkatraghavan et al.<sup>42</sup> showing marked fluctuations in brain BOLD in 4 patients undergoing propofol anaesthesia with intracranial steal using a similar CO<sub>2</sub> ramp protocol as in this study, indicating that the CO<sub>2</sub> responsiveness we describe in the awake state persists under anaesthesia. Also well-known is the rapid response by the brain to alterations in ET CO<sub>2</sub> to

control intracranial volume during anaesthesia for neurosurgical procedures. We have previously demonstrated that intraoperative hypocapnia is associated with an increased incidence of POND,<sup>23</sup> however, ET O<sub>2</sub> fluctuations were not considered as a potential factor in that study. The results of the present study suggest both O<sub>2</sub> and CO<sub>2</sub> changes may be important. MacDonald et al.<sup>43</sup> reported variations in CBF of nearly 100% in 10 healthy subjects exposed to hyperoxia. This heterogeneity of regional responses to hyperoxia suggests that one CBF does not fit all regions, either in grey or white matter. Thus, each individual may have a unique CBF response during surgery with great regional heterogeneity as the ET gases are manipulated. Other human studies have indicated that hyperoxia induces cerebral vasoconstriction as a consequence of altered regional nitric oxide potentially contributing to the stress diathesis under anaesthesia.<sup>44</sup> Also of note are findings of altered CVR with increasing age<sup>45</sup> and with signs of dementia in the elderly<sup>46</sup> or in patients with biomarkers such as APO4ε related to early onset Alzheimer's disease.<sup>47</sup> The identification of regional 'intracranial steal' or 'blue brain' on the BOLD images with a CO<sub>2</sub> ramp protocol is increasingly being used to establish the need for and measure results from revascularization with superficial temporal artery to middle cerebral artery (STA-MCA) anastomoses in patients with severe intracranial vascular compromise.<sup>48,49</sup> Such patients when successfully revascularised see improvements in CVR and complete or partial resolution of the 'blue brain' signal that indicated the area of regional steal. Thus, these abnormal regions as identified in our study have clear pathological correlates. There are currently no comparable studies regarding O<sub>2</sub> ramp protocols and the 'blue brain' seen in this study with this imaging protocol but analogies to the findings with the CO<sub>2</sub> ramp protocol are envisioned. Also, importantly not addressed here is the potential findings of an O<sub>2</sub> ramp protocol in the presence of a clamped period of hypocapnia. It is this sequence that is especially interesting as this respiratory gas profile is common during anaesthesia. The short hypocapnic periods obtained in this study were obtained by having the subject spontaneously hyperventilating on command. An 11-minute ramp sequence with stable hypocapnia by spontaneous hyperventilation for such a duration is not feasible in awake subjects. That said our 3<sup>rd</sup> pCASL sequence in 4 subjects where a 3-minute period of hyperoxia with hypocapnia indicates a synergic diffuse decrease in CBF which potentially could have deleterious effects in patients at risk of POND.

Based on these initial observations we advance the hypothesis that end-tidal respiratory gas control is a critical management consideration during anaesthesia; a much more important consideration than previously thought. Older patients appear to be at greater risk of 'intracranial steal' of regional CBF with alterations in CO<sub>2</sub> and O<sub>2</sub>. Our previous study confirms an association between CO<sub>2</sub> management and POND.<sup>23,32</sup> The imaging in the present study suggests that a combination of hyperoxia and hypocapnia may be particularly worrisome. We suggest that anaesthetic management may be optimized for cerebral health by attempting to maintain respiratory gases at or near the patient baseline values to stabilize CBF during the conduct of anaesthesia. An exception may occur during neurosurgical procedures where deliberate alterations to lower ET CO<sub>2</sub> may be required. The marked CBF fluctuations as seen with controlled ET gas manipulation in this study imply that such CBF changes can occur under anaesthesia where similar changes in ET gases routinely occur. Such large alterations in CBF and oxygenation may be a contributing factor to the development of POND in susceptible individuals. A clinical trial comparing rigorous

maintenance of end-tidal gases at a patient's own baseline, to standard anaesthetic management to determine if the changes in CBF and oxygenation as seen in awake subjects in this study have an influence on the development of POND could be considered.

**Acknowledgements:**

The authors thank Dr. Joseph Fisher, Dr. James Duffin and Dr. David Mikulis, developers of the RespirAct used in these studies for helpful discussions about the methodological approach used here for ET gas control.

**Authors Contributions:**

WACM: Funding, conception of the study, recruitment, conduct of the study, data collation, data processing, analysis, writing

REL-G: Funding, conception of the study, data collation, data processing, analysis, writing

LR: Conception of the study, data collation, data processing, analysis, writing

JP: Recruitment, conduct of the study, data collation, data processing, analysis, writing

ME: Funding, conception of the study, analysis, writing

KK: Recruitment, conduct of the study, data collation, data processing, writing

KF: Recruitment, conduct of the study, data collation, data processing, writing

MRG: Funding, conception of the study, data collation, data processing, analysis, writing

## Legends to Figures:

**Figure 1 A-C:** A: BOLD response to the CO<sub>2</sub> ramp with the ETO<sub>2</sub> tension clamped at ~100 mmHg. The expected response with increased BOLD signal to the ramp stimulus is depicted by orange voxels. A diffuse response is seen. The scale is t-scores based on fit to the GLM from SPM first level analysis. The blue voxels depict the inverse response. The t-score had to exceed 3.11 (p=0.001) to be colourized. B: The response of one voxel to the CO<sub>2</sub> ramp. The incremental and rapid increase with the step change in CO<sub>2</sub> (grey scale) is seen by the red dots representing the BOLD scan signal intensity at that moment in time. C: The inverse response of one voxel to the CO<sub>2</sub> ramp. The incremental and rapid decrease with the step change in CO<sub>2</sub> (grey scale) is seen by the red dots representing the BOLD scan signal intensity at that moment in time.

**Figure 2 A-C:** BOLD response to the O<sub>2</sub> ramp with the ETCO<sub>2</sub> tension clamped at ~43 mmHg. The expected response to the ramp stimulus is depicted by orange voxels. A diffuse response is seen. The scale is t-scores based on fit to the GLM from SPM first level analysis. The blue voxels depict the inverse response. The t-score had to exceed 3.11 (p=0.001) to be colourized. B: The response of one voxel to the O<sub>2</sub> ramp. The incremental and rapid increase with the step change in O<sub>2</sub> (grey scale) is seen by the red dots representing the BOLD scan signal intensity at that moment in time. C: The inverse response of one voxel to the O<sub>2</sub> ramp. The incremental and rapid decrease with the step change in O<sub>2</sub> (grey scale) is seen by the red dots representing the BOLD scan signal intensity at that moment in time.

**Figure 3:** Graph of the relationship between inverse voxels to CO<sub>2</sub> and O<sub>2</sub> and age. The data best fit a 2<sup>nd</sup> order polynomial; p=0.019. A representative example in one patient following 2<sup>nd</sup> level analysis showing the less than response to the CO<sub>2</sub> ramp stimulus (in red) and the less than response to the O<sub>2</sub> ramp stimulus (in blue) with a leave-one-out analysis (removing this subject and comparing this subject to the other 11 subjects).

**Figure 4 A-C:** Dynamism of the response of CBF to alterations in ET gases. A: CVR difference map of hypercapnia – baseline settings at normoxia. B: CVR difference of hyperoxia – baseline settings at normocapnia, C: CVR difference of hyperoxia/hypocapnia – baseline. Such a situation is often present during anaesthesia. The large decrement in regional CBF is essentially universally evident.

**Figure 5A and B:** A single slice at -8 mm below the AC-PC line to show the relationship between BOLD response to hyperoxia and the changes in CBF under these conditions. The heterogeneity of response is evident as is the correlation of decreased BOLD (inverse response) and decreased CBF in regions of the frontal cortex, depicted by the purple arrows. The scales for the BOLD image are t-scores as described above. The scale for the CBF results is  $\pm$  flow mg/g/min.

**Supplemental File 1:** Display of the end-tidal gas control as described in Methods for one subject.

**Supplemental File 2:** Description of the MRI sequences used in the study.

**Supplemental File 3:** Single subject mask (individualized based on their imaging) with B0 inhomogeneities masked out and a CSF ventricular mask included at 1-fold dilation as determined from the WFU pick atlas. In this manner potential BOLD signal error were removed from areas adjacent to surface transitions were not included in the voxel analysis at the 1<sup>st</sup> and 2<sup>nd</sup> levels.

**Supplemental File 4:** 2<sup>nd</sup> level group analysis based on the inverse response to the O<sub>2</sub> ramp (orange voxels) and the inverse response to the CO<sub>2</sub> ramp (blue voxels) at the p = 0.01 level. The groups were 4 older subjects age (53-62) with voxel counts above 50 at the p = 0.001 level from Table 5 and 6. The 'control group' was the other 8 subjects (mean age 43 ± 13). The distribution of blue voxels showing the group response of a greater voxel count to the inverse CO<sub>2</sub> stimulus is similar to that seen in reference 23 and identified as a biomarker of POND in this previous work.

## References:

1. Evered, L. *et al.* Recommendations for the Nomenclature of Cognitive Change Associated with Anaesthesia and Surgery-2018. *J. Alzheimers. Dis.* **66**, 1–10 (2018).
2. Leslie, D. L., Marcantonio, E. R., Zhang, Y., Leo-Summers, L. & Inouye, S. K. One-year health care costs associated with delirium in the elderly population. *Arch. Intern. Med.* **168**, 27–32 (2008).
3. Gross, A. L. *et al.* Delirium and Long-term Cognitive Trajectory Among Persons With Dementia. *Arch. Intern. Med.* **172**, 1324–31 (2012).
4. Inouye, S. K., Westendorp, R. G. J. & Saczynski, J. S. Delirium in elderly people. *Lancet (London, England)* **383**, 911–22 (2014).
5. Bilotta, F., Evered, L. A. & Gruenbaum, S. E. Neurotoxicity of anesthetic drugs: an update. *Curr. Opin. Anaesthesiol.* **30**, 452–457 (2017).
6. Vinson, A. E. & Houck, C. S. Neurotoxicity of Anesthesia in Children: Prevention and Treatment. *Curr. Treat. Options Neurol.* **20**, 51 (2018).
7. Fu, H., Fan, L. & Wang, T. Perioperative neurocognition in elderly patients. *Curr. Opin. Anaesthesiol.* **31**, 24–29 (2018).
8. Johnson, S. C., Pan, A., Li, L., Sedensky, M. & Morgan, P. Neurotoxicity of anesthetics: Mechanisms and meaning from mouse intervention studies. *Neurotoxicol. Teratol.* **71**, 22–31
9. Jevtovic-Todorovic, V. General Anesthetics and Neurotoxicity: How Much Do We Know? *Anesthesiol. Clin.* **34**, 439–451 (2016).
10. Coleman, K. *et al.* Isoflurane Anesthesia Has Long-term Consequences on Motor and Behavioral Development in Infant Rhesus Macaques. *Anesthesiology* **126**, 74–84 (2017).
11. Raper, J., Alvarado, M. C., Murphy, K. L. & Baxter, M. G. Multiple Anesthetic Exposure in Infant Monkeys Alters Emotional Reactivity to an Acute Stressor. *Anesthesiology* **123**, 1084–92 (2015).
12. Raper, J., De Biasio, J. C., Murphy, K. L., Alvarado, M. C. & Baxter, M. G. Persistent alteration in behavioural reactivity to a mild social stressor in rhesus monkeys repeatedly exposed to sevoflurane in infancy. *Br. J. Anaesth.* **120**, 761–767 (2018).
13. Mutch, W. A. C., El-Gabalawy, R. M. & Graham, M. R. Postoperative Delirium, Learning, and Anesthetic Neurotoxicity: Some Perspectives and Directions. *Front. Neurol.* **9**, 177 (2018).
14. Mutch, W. A. C. & El-Gabalawy, R. Anesthesia and postoperative delirium: the agent is a strawman - the problem is CO<sub>2</sub>. *Can. J. Anaesth.* (2017). doi:10.1007/s12630-017-0859-3
15. Graham, M. R. The hydra of anesthetic neurotoxicity: Myth or reality? *Paediatr. Anaesth.* **28**, 576–577 (2018).
16. Warner, D. O. *et al.* Neuropsychological and Behavioral Outcomes after Exposure of Young Children to Procedures Requiring General Anesthesia: The Mayo Anesthesia Safety in Kids (MASK) Study. *Anesthesiology* **129**, 89–105 (2018).
17. Wildes, T. S. *et al.* Effect of Electroencephalography-Guided Anesthetic Administration on Postoperative Delirium Among Older Adults Undergoing Major Surgery: The ENGAGES Randomized Clinical Trial. *JAMA* **321**, 473–483 (2019).
18. Saxena, S. & Maze, M. Impact on the brain of the inflammatory response to surgery. *Presse Med.* **47**, e73–e81 (2018).
19. Cortese, G. P. & Burger, C. Neuroinflammatory challenges compromise neuronal function in the aging brain: Postoperative cognitive delirium and Alzheimer’s disease. *Behav. Brain Res.* **322**, 269–279 (2017).
20. Wang, Y. & Shen, X. Postoperative delirium in the elderly: the potential neuropathogenesis. *Aging Clin. Exp. Res.* **30**, 1287–1295 (2018).
21. Fong, T. G. *et al.* Delirium accelerates cognitive decline in Alzheimer disease. *Neurology* **72**, 1570–5 (2009).
22. Inouye, S. K. Delirium in older persons. *N.Engl.J.Med.* **354**, 1157–1165 (2006).
23. El-Gabalawy, R. *et al.* A novel stress-diathesis model to predict risk of post-operative delirium: Implications for intra-operative management. *Front. Aging Neurosci.* **9**, (2017).
24. Mutch, W. A. C. *et al.* Approaches to Brain Stress Testing: BOLD Magnetic Resonance Imaging with Computer-Controlled Delivery of Carbon Dioxide. *PLoS One* **7**, (2012).
25. Fierstra, J. *et al.* Measuring cerebrovascular reactivity: what stimulus to use? *J. Physiol.* **591**, 5809–21 (2013).
26. Slessarev, M. *et al.* Prospective targeting and control of end-tidal CO<sub>2</sub> and O<sub>2</sub> concentrations. *J. Physiol.* **581**, 1207–1219 (2007).
27. Fisher, J. A., Iscoe, S. & Duffin, J. Sequential gas delivery provides precise control of alveolar gas exchange. *Respir. Physiol. Neurobiol.* **225**, 60–69 (2016).

28. Wang, Z. *et al.* Empirical optimization of ASL data analysis using an ASL data processing toolbox: ASLtbx. *Magn. Reson. Imaging* **26**, 261–9 (2008).
29. Ellis, M. J. *et al.* Neuroimaging assessment of cerebrovascular reactivity in concussion: Current concepts, methodological considerations, and review of the literature. *Front. Neurol.* **7**, 1–16 (2016).
30. Mutch, W. A. C. *et al.* Patient-specific alterations in CO<sub>2</sub> cerebrovascular responsiveness in acute and sub-acute sports-related concussion. *Front. Neurol.* **9**, (2018).
31. Ellis, M. J. *et al.* Brain magnetic resonance imaging CO<sub>2</sub> stress testing in adolescent postconcussion syndrome. *J. Neurosurg.* **125**, (2016).
32. Mutch, W. A. C., El-Gabalawy, R., Girling, L., Kilborn, K. & Jacobsohn, E. End-Tidal Hypocapnia Under Anesthesia Predicts Postoperative Delirium. *Front. Neurol.* **9**, 678 (2018).
33. Dony, P., Dramaix, M. & Boogaerts, J. G. Hypocapnia measured by end-tidal carbon dioxide tension during anesthesia is associated with increased 30-day mortality rate. *J. Clin. Anesth.* **36**, 123–126 (2017).
34. Akkermans, A. *et al.* An observational study of end-tidal carbon dioxide trends in general anesthesia. *Can. J. Anaesth.* **66**, 149–160 (2019).
35. Duffin, J. *et al.* Cerebrovascular resistance: the basis of cerebrovascular reactivity. *Front. Neurosci.* **12**, 409 (2018).
36. Kim, S.-G. & Ogawa, S. Biophysical and physiological origins of blood oxygenation level-dependent fMRI signals. *J. Cereb. Blood Flow Metab.* **32**, 1188–206 (2012).
37. Mutch, W. A. *et al.* Cerebral hypoxia during cardiopulmonary bypass: a magnetic resonance imaging study. *Ann.Thorac.Surg.* **64**, 695–701 (1997).
38. Arendash, G. W. *et al.* Oxygen treatment triggers cognitive impairment in Alzheimer’s transgenic mice. *Neuroreport* **20**, 1087–92 (2009).
39. Arendash, G. W., Su, G. C., Crawford, F. C., Bjugstad, K. B. & Mullan, M. Intravascular beta-amyloid infusion increases blood pressure: implications for a vasoactive role of beta-amyloid in the pathogenesis of Alzheimer’s disease. *Neurosci. Lett.* **268**, 17–20 (1999).
40. Zhilyaev, S. Y. *et al.* Hyperoxic vasoconstriction in the brain is mediated by inactivation of nitric oxide by superoxide anions. *Neurosci. Behav. Physiol.* **33**, 783–7 (2003).
41. Liu, P. *et al.* Multiparametric imaging of brain hemodynamics and function using gas-inhalation MRI. *Neuroimage* 0–1 (2016). doi:10.1016/j.neuroimage.2016.09.063
42. Venkatraghavan, L. *et al.* Measurement of Cerebrovascular Reactivity as Blood Oxygen Level-Dependent Magnetic Resonance Imaging Signal Response to a Hypercapnic Stimulus in Mechanically Ventilated Patients. *J. Stroke Cerebrovasc. Dis.* **27**, 301–308 (2018).
43. MacDonald, M. E., Berman, A. J. L., Mazerolle, E. L., Williams, R. J. & Pike, G. B. Modeling hyperoxia-induced BOLD signal dynamics to estimate cerebral blood flow, volume and mean transit time. *Neuroimage* **178**, 461–474 (2018).
44. Mattos, J. D. *et al.* Human brain blood flow and metabolism during isocapnic hyperoxia: the role of reactive oxygen species. *J. Physiol.* **597**, 741–755 (2019).
45. McKetton, L. *et al.* The aging brain and cerebrovascular reactivity. *Neuroimage* **181**, 132–141 (2018).
46. van der Thiel, M., Rodriguez, C., Van De Ville, D., Giannakopoulos, P. & Haller, S. Regional Cerebral Perfusion and Cerebrovascular Reactivity in Elderly Controls With Subtle Cognitive Deficits. *Front. Aging Neurosci.* **11**, 19 (2019).
47. Wolters, F. J. *et al.* Cerebral Vasoreactivity, Apolipoprotein E, and the Risk of Dementia: A Population-Based Study. *Arterioscler. Thromb. Vasc. Biol.* **36**, 204–10 (2016).
48. Rosen, C. *et al.* Long-term changes in cerebrovascular reactivity following EC-IC bypass for intracranial steno-occlusive disease. *J. Clin. Neurosci.* **54**, 77–82 (2018).
49. Sam, K. *et al.* Assessing the effect of unilateral cerebral revascularisation on the vascular reactivity of the non-intervened hemisphere: a retrospective observational study. *BMJ Open* **5**, e006014 (2015).

## Table 1

### Subject Demographics

Study #	Age	Sex	Status	Medications	Resting BP
1	42	M	Migraines	Nil	122/77
2	29	M	Remote concussion	Nil	118/69
3	61	F	Healthy	Antibiotics	135/83
4	45	M	Healthy	Nil	138/86
5	57	F	Healthy	Nil	141/89
6	53	F	Healthy	Nil	145/77
7	62	M	Healthy	Nil	155/84
8	44	M	Healthy	Nil	110/70
9	20	F	Healthy	Nil	110/66
10	54	F	Healthy	Nil	130/82
11	56	F	Healthy	Nil	138/74
12	52	F	Healthy	Nil	112/65

**Table 2**  
**End-tidal Gas Targeting**

Study #	Baseline CO2	Hypocapnic CO2	Ramp Peak		
			CO2	O2	
1	45.5	41.2	53.0	103.5	534.0
2	40.2	35.5	50.1	110.0	411.0
3	37.8	31.0	46.6	102.5	489.0
4	38.1	32.3	45.2	99.7	461.0
5	43.2	38.3	53.1	101.8	427.0
6	41.7	36.6	51.9	100.1	461.0
7	40.9	37.6	53.1	110.2	415.0
8	48.1	43.4	57.4	99.8	409.0
9	40.8	36.9	49.0	104.2	463.0
10	42.9	37.1	53.8	101.9	522.0
11	41.6	38.6	51.2	101.5	541.0
12	43.1	38.9	52.1	99.5	565.0
<b>Mean</b>	<b>42.0</b>	<b>37.3</b>	<b>51.4</b>	<b>102.9</b>	<b>474.8</b>
<b>SD</b>	<b>2.9</b>	<b>3.4</b>	<b>3.3</b>	<b>3.7</b>	<b>55.0</b>

### Table 3

#### 1<sup>st</sup> Level Analysis CO<sub>2</sub> Ramp

Subject	Raw Voxel Counts			Masked Voxel Counts			Imaged p = 1.0	%ResponseMasked	
	Hyper	Inv	Total	Hyper	Inv	Total		Hyper	Inv
1	171535	664	172199	165194	164	165358	188356	87.8	0.1
2	176211	1088	177299	169377	614	169991	191764	88.6	0.4
3	149610	475	150085	144360	460	144820	171395	84.5	0.3
4	147991	0	147991	141345	0	141345	175213	80.7	0.0
5	140787	879	141666	136393	528	136921	163827	83.6	0.4
6	143022	4556	147578	138784	2881	141665	180009	78.7	2.0
7	135339	118	135457	130415	56	130471	165881	78.7	0.0
8	136464	466	136930	129637	310	129947	162218	80.1	0.2
9	162694	1442	164136	157492	648	158140	189248	83.6	0.4
10	165279	294	165573	157291	244	157535	178274	88.4	0.2
11	155785	1225	157010	148335	847	149182	175290	85.1	0.6
12	147928	1750	149678	143464	857	144321	170293	84.7	0.6
<b>Mean</b>	<b>152720</b>	<b>1080</b>	<b>153800</b>	<b>146841</b>	<b>634</b>	<b>147475</b>	<b>175981</b>	<b>83.7</b>	<b>0.4</b>
<b>SD</b>	<b>13586</b>	<b>1219</b>	<b>13545</b>	<b>12994</b>	<b>763</b>	<b>12936</b>	<b>9970</b>	<b>3.6</b>	<b>0.5</b>

Hyper - expected GLM fit to CO<sub>2</sub> ramp

Inv - inverse response GLM fit to CO<sub>2</sub> ramp

p = 0.001

Raw voxel counts - grey matter + white matter inclusive mask

Masked voxel counts - mask as in Supplemental File 3

Total with p = 1.0 - all voxels

imaged/patient

## Table 4

### 1<sup>st</sup> Level Analysis O<sub>2</sub> Ramp

Subject	Raw Voxel Counts			Masked Voxel Counts			Imaged p = 1.0	%ResponseMasked	
	Hyper	Inv	Total	Hyper	Inv	Total		Hyper	Inv
1	167536	1018	168554	161574	411	161985	189485	85.3	0.2
2	162894	37	162931	156581	0	156581	192232	81.5	0.0
3	104446	10378	114824	101379	8882	110261	172364	58.8	5.2
4	164438	49	164487	156126	41	156167	174910	89.3	0.0
5	158102	1280	159382	151166	882	152048	165354	91.4	0.5
6	161567	5672	167239	154975	3895	158870	179049	86.6	2.2
7	143566	4326	147892	138870	2949	141819	166975	83.2	1.8
8	146776	618	147394	138662	138	138800	162406	85.4	0.1
9	175849	1432	177281	168717	726	169443	189268	89.1	0.4
10	163619	6699	170318	155999	3478	159477	179612	86.9	1.9
11	160986	3395	164381	154632	1236	155868	175470	88.1	0.7
12	158532	1409	159941	151934	917	152851	170872	88.9	0.5
<b>Mean</b>	<b>155693</b>	<b>3026</b>	<b>158719</b>	<b>149218</b>	<b>1963</b>	<b>151181</b>	<b>176500</b>	<b>84.5</b>	<b>1.1</b>
<b>SD</b>	<b>18258</b>	<b>3194</b>	<b>16253</b>	<b>17219</b>	<b>2567</b>	<b>15294</b>	<b>9822</b>	<b>8.6</b>	<b>1.5</b>

Hyper - expected GLM fit to O<sub>2</sub> ramp

Inv - inverse response GLM fit to O<sub>2</sub> ramp

p = 0.001

Raw voxel counts - grey matter + white matter inclusive mask

Masked voxel counts - mask as in Supplemental File 3

Total with p = 1.0 - all voxels

imaged/patient

## Table 5

### 2<sup>nd</sup> Level Analysis CO<sub>2</sub> Ramp

Subject	Raw Voxel Counts			Masked Voxel Counts			Imaged p = 1.0	%ResponseMasked	
	> Group	< Group	Total	> Group	< Group	Total		> Group	< Group
1	3172	0	3172	2874	0	2874	188356	1.5	0.00
2	1133	0	1133	1098	0	1098	191764	0.6	0.00
3	148	22	170	143	22	165	171395	0.1	0.01
4	1025	10	1035	892	0	892	175213	0.5	0.00
5	94	11	105	83	11	94	163827	0.1	0.01
6	35	242	277	11	118	129	180009	0.0	0.07
7	0	13	13	0	10	10	165881	0.0	0.01
8	8090	77	8167	7436	46	7482	162218	4.6	0.03
9	2067	10	2077	1978	10	1988	189248	1.0	0.01
10	485	24	509	444	24	468	178274	0.2	0.01
11	117	80	197	101	18	119	175290	0.1	0.01
12	223	0	223	204	0	204	170293	0.1	0.00
<b>Mean</b>	<b>1382</b>	<b>41</b>	<b>1423</b>	<b>1272</b>	<b>22</b>	<b>1294</b>	<b>175981</b>	<b>0.7</b>	<b>0.01</b>
<b>SD</b>	<b>2326</b>	<b>69</b>	<b>2328</b>	<b>2139</b>	<b>33</b>	<b>2141</b>	<b>9970</b>	<b>1.3</b>	<b>0.02</b>

Leave-one-out analysis

> Group - Subject greater voxel counts than Group

< Group - Subject less voxel counts than Group

p < 0.001

Raw voxel counts - grey matter + white matter inclusive mask

Masked voxel counts - mask as in Supplemental File 3

Total with p = 1.0 - all voxels

imaged/patient

## Table 6

### 2<sup>nd</sup> Level Analysis O<sub>2</sub> Ramp

Subject	Raw Voxel Counts			Masked Voxel Counts			Imaged p = 1.0	%ResponseMasked	
	> Group	< Group	Total	> Group	< Group	Total		> Group	< Group
1	96	0	96	91	0	91	189485	0.0	0.00
2	1019	0	1019	990	0	990	192232	0.5	0.00
3	0	1026	1026	0	912	912	172364	0.0	0.53
4	5277	10	5287	4807	0	4807	174910	2.7	0.00
5	247	0	247	182	0	182	165354	0.1	0.00
6	211	297	508	176	74	250	179049	0.1	0.04
7	190	68	258	176	54	230	166975	0.1	0.03
8	4530	0	4530	3997	0	3997	162406	2.5	0.00
9	67	0	67	67	0	67	189268	0.0	0.00
10	39	131	170	29	102	131	179612	0.0	0.06
11	43	0	43	32	0	32	175470	0.0	0.00
12	115	0	115	107	0	107	170872	0.1	0.00
<b>Mean</b>	<b>986</b>	<b>128</b>	<b>1114</b>	<b>888</b>	<b>95</b>	<b>983</b>	<b>176500</b>	<b>0.5</b>	<b>0.05</b>
<b>SD</b>	<b>1856</b>	<b>297</b>	<b>1812</b>	<b>1671</b>	<b>260</b>	<b>1637</b>	<b>9822</b>	<b>1.0</b>	<b>0.15</b>

Leave-one-out analysis

> Group - Subject greater voxel counts than Group

< Group - Subject less voxel counts than Group

p < 0.001

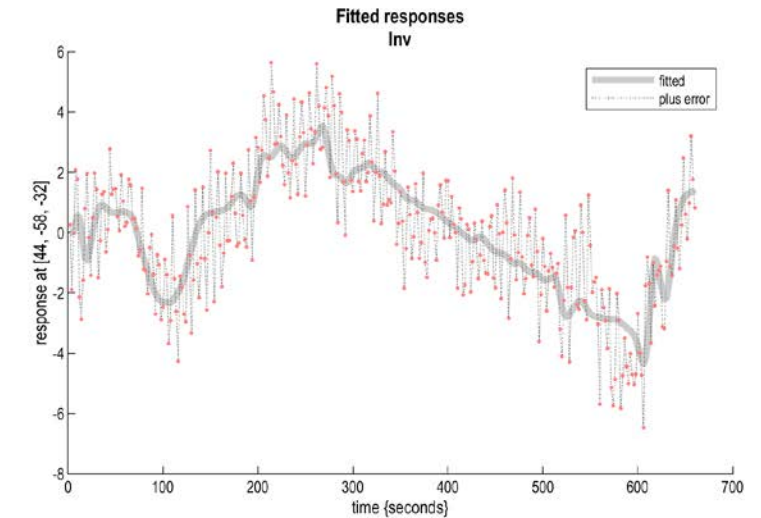
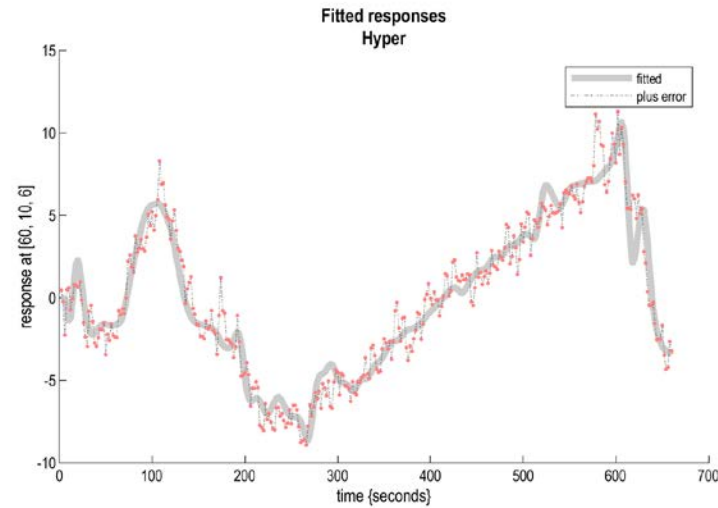
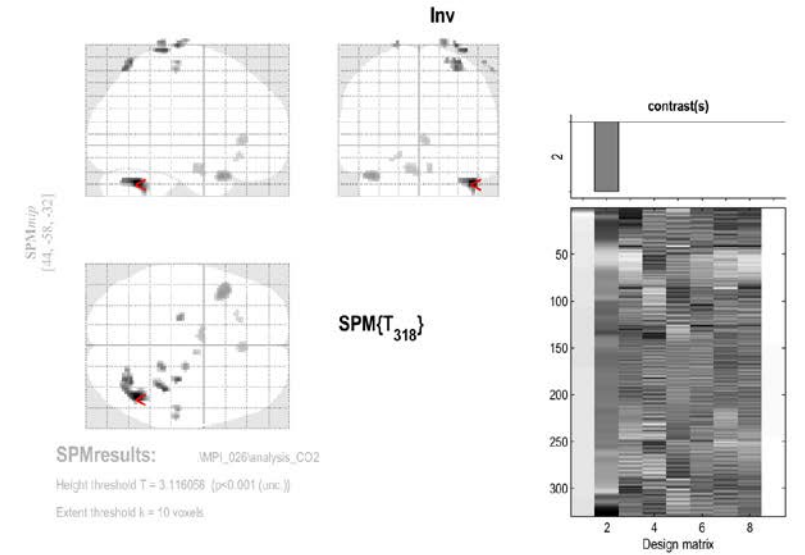
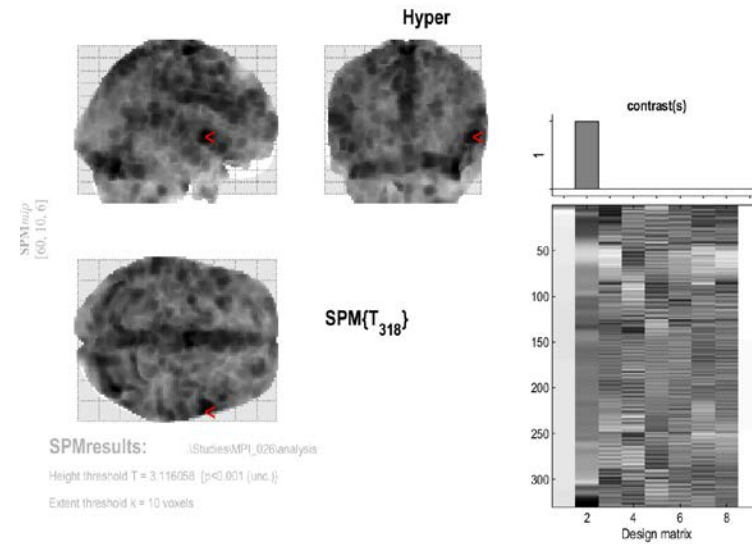
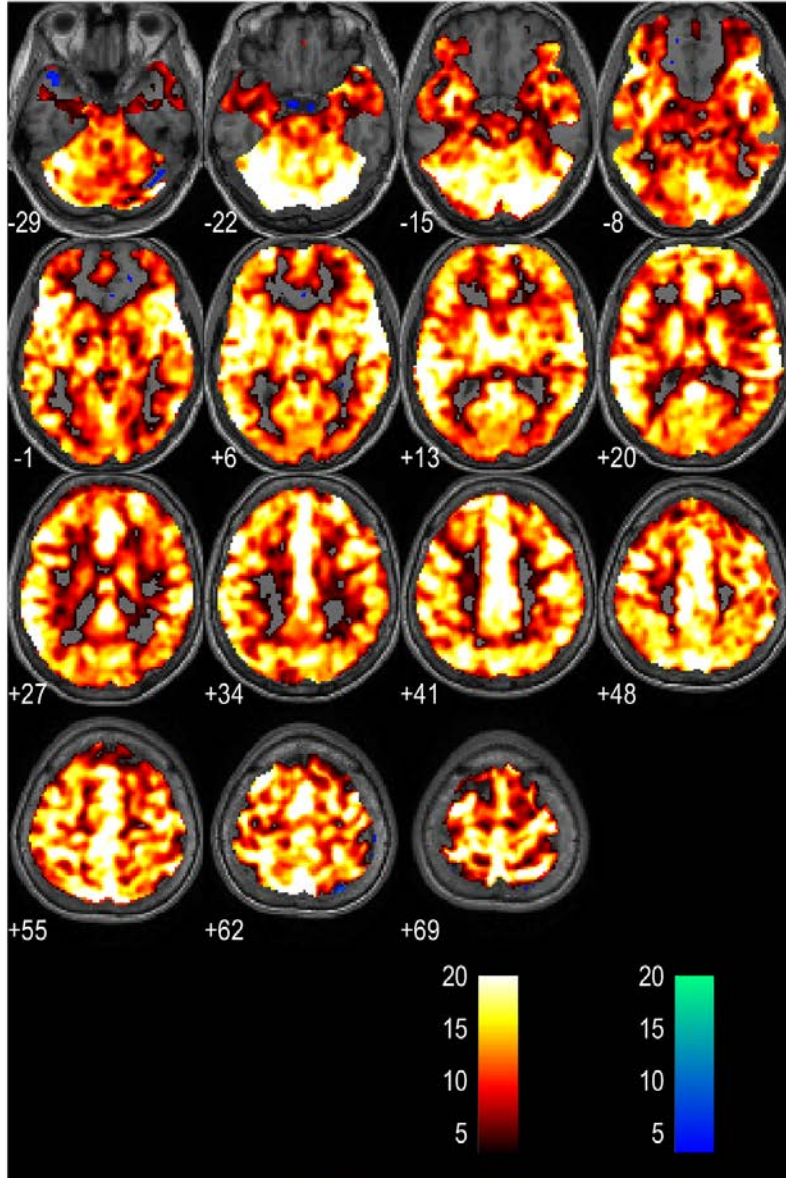
Raw voxel counts - grey matter + white matter inclusive mask

Masked voxel counts - mask as in Supplemental File 3

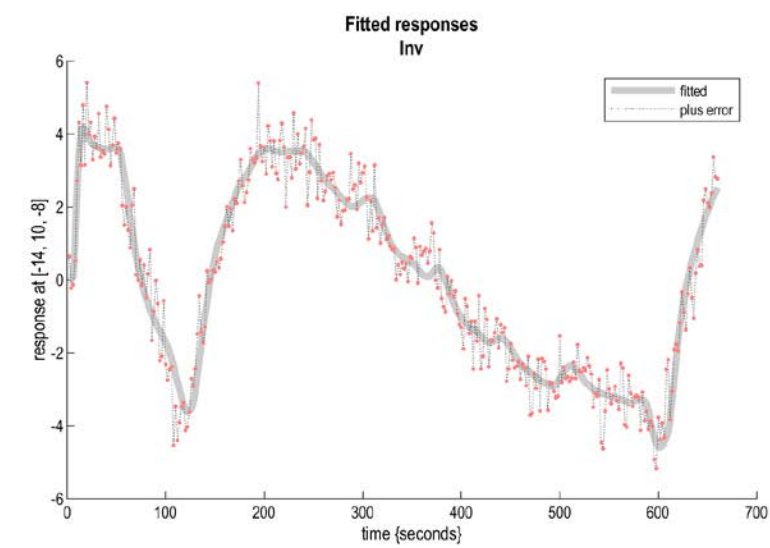
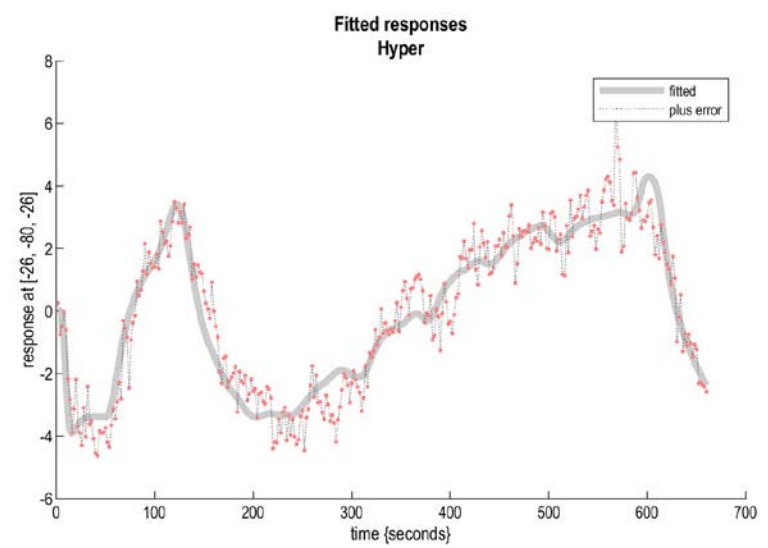
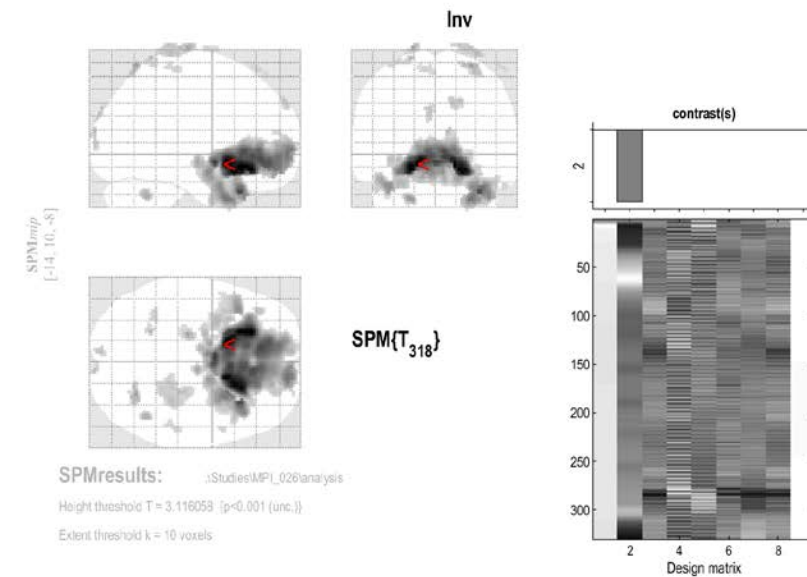
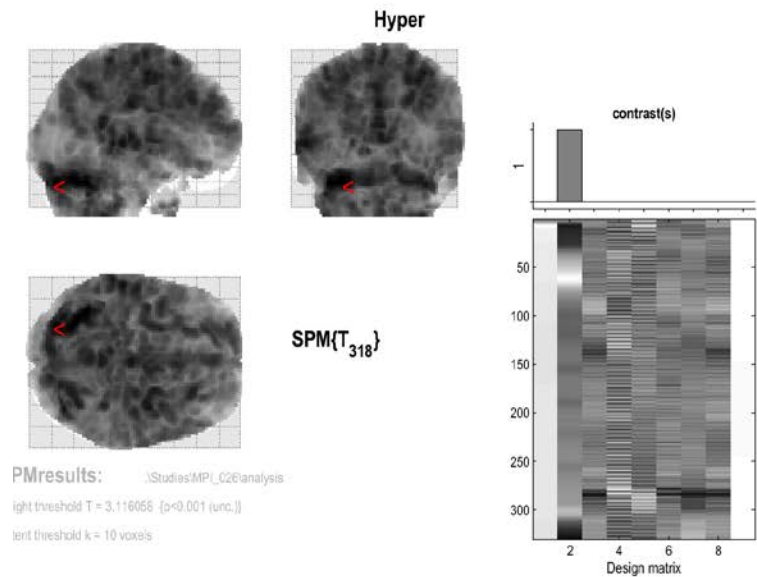
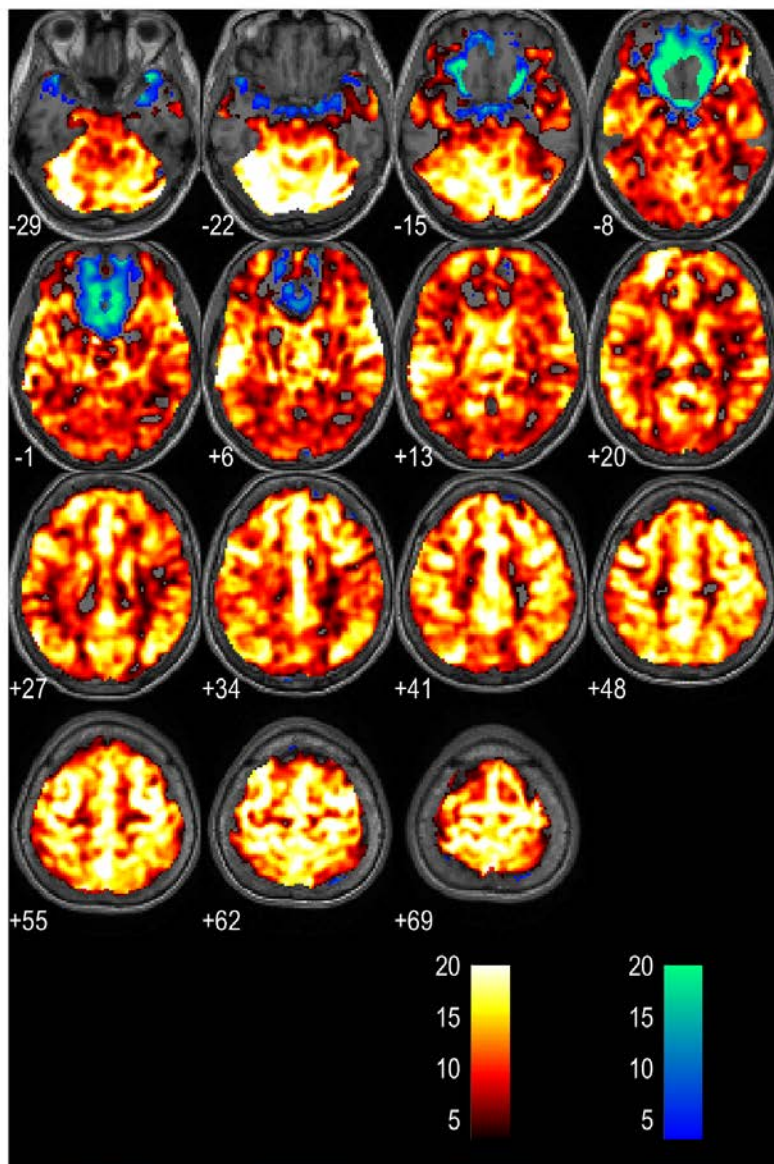
Total with p = 1.0 - all voxels

imaged/patient

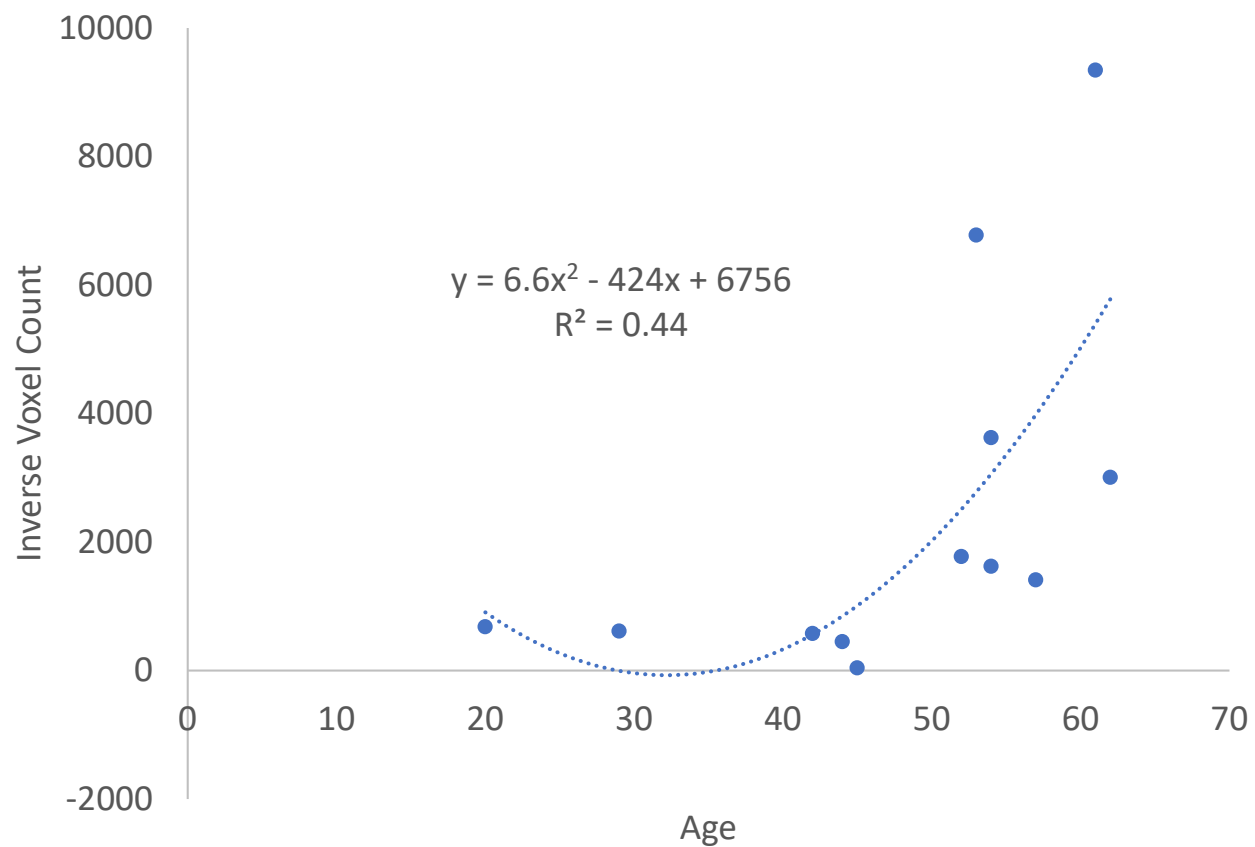
# BOLD response to CO<sub>2</sub> ramp



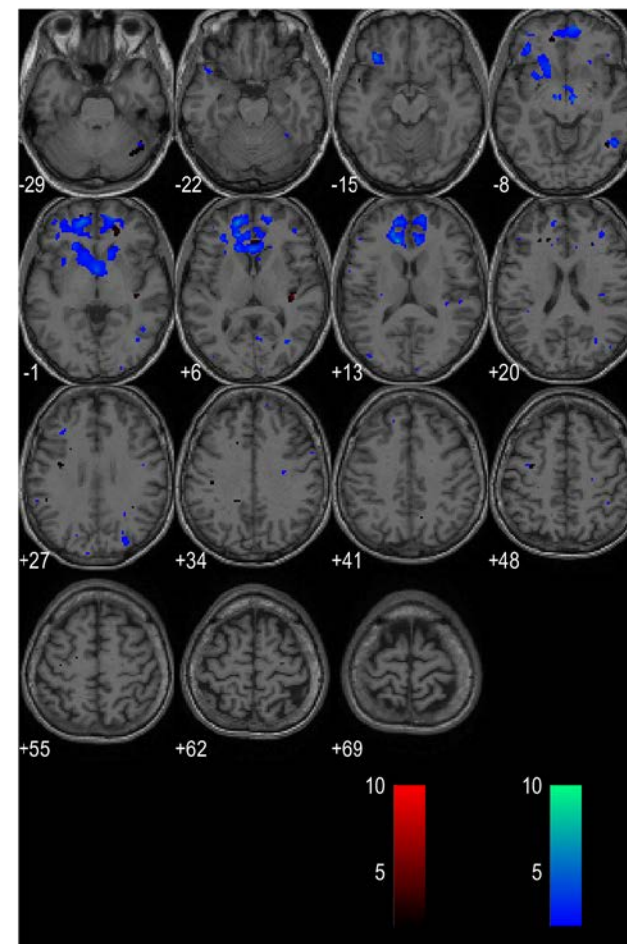
# BOLD response to O<sub>2</sub> ramp



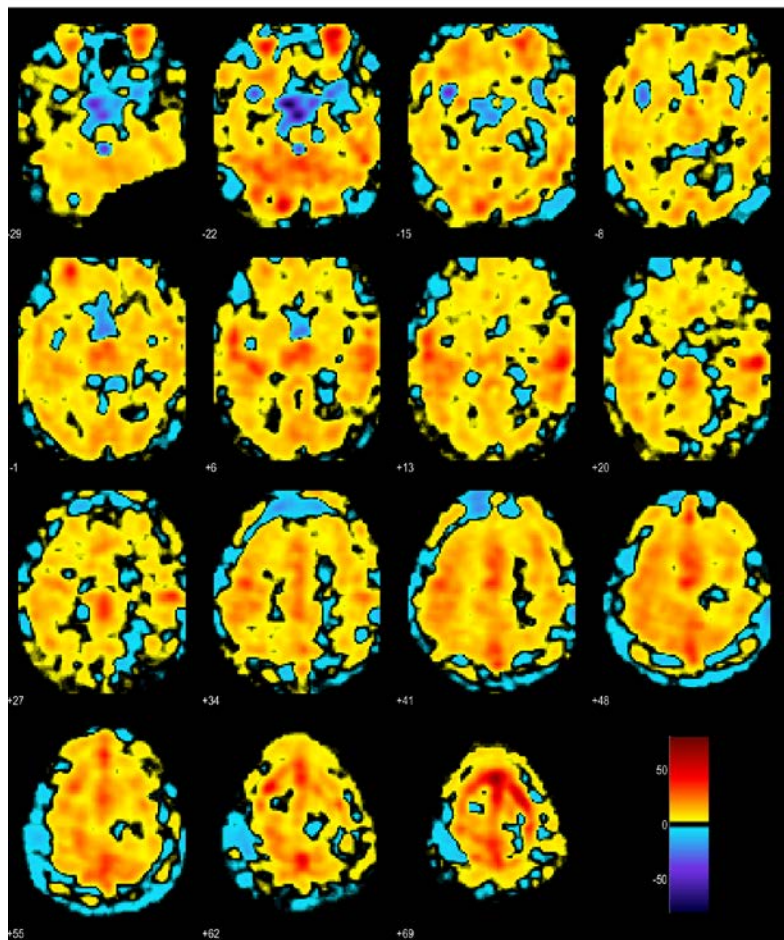
# Inverse Response Voxel Count to Ramp Stimulus



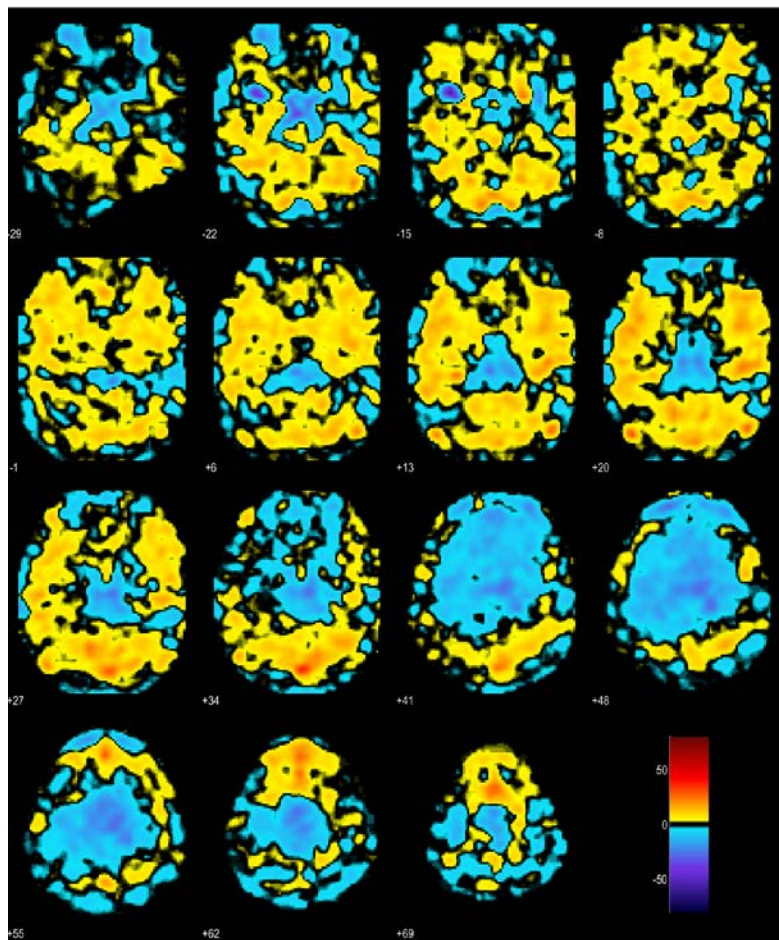
# Subject inverse response to O<sub>2</sub> and CO<sub>2</sub> Ramps



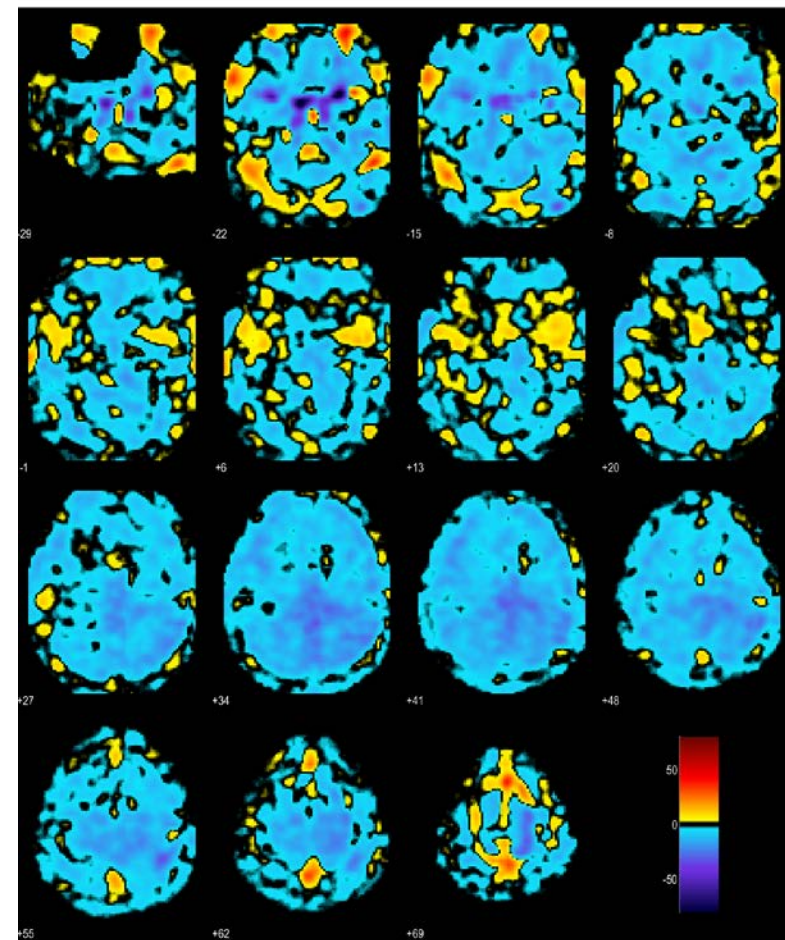
# pCASL CVR responses to altered ETCO<sub>2</sub> and O<sub>2</sub>



Hypercapnia – BL

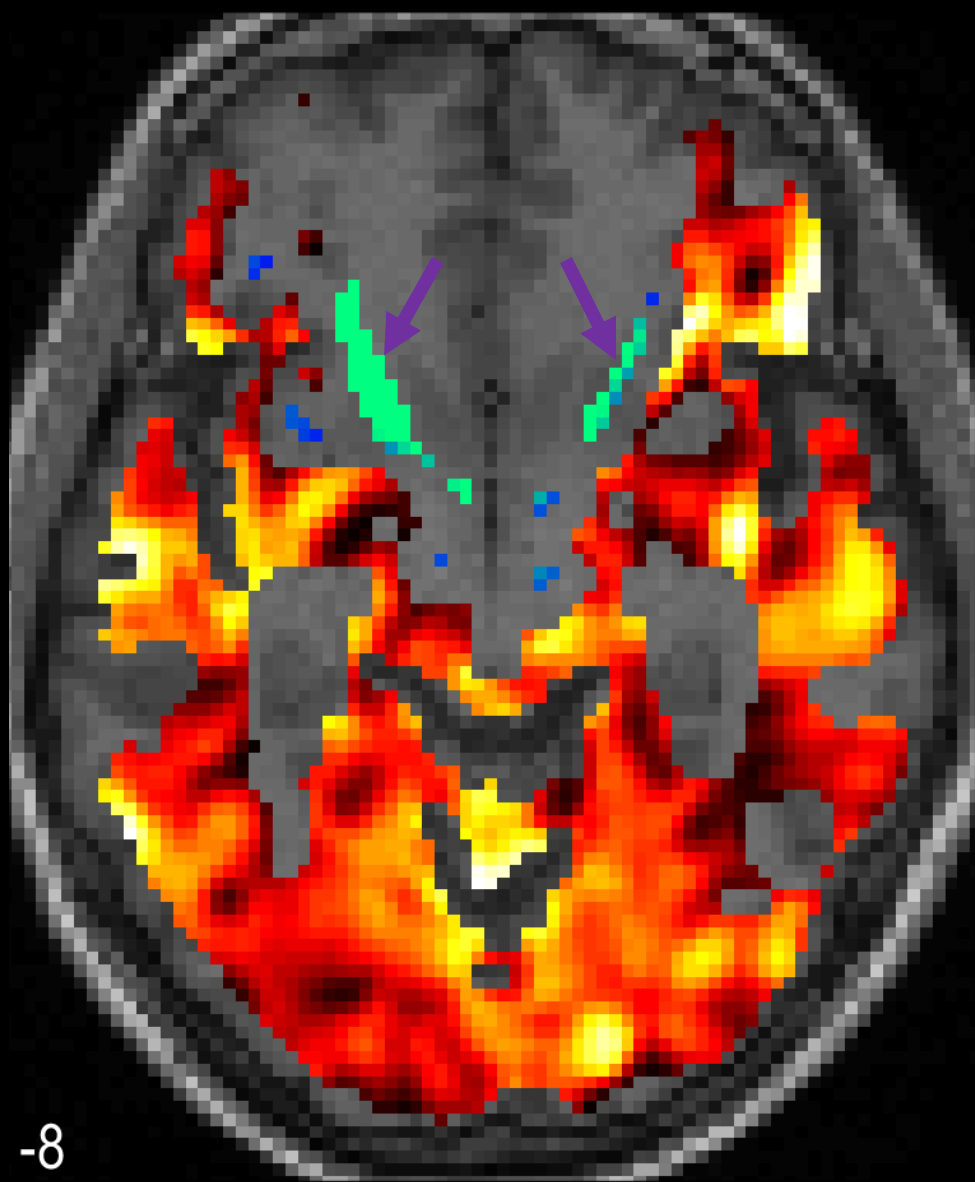


Hyperoxia – BL

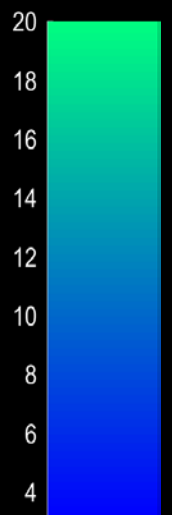


Hyperoxia + Hypocapnia - BL

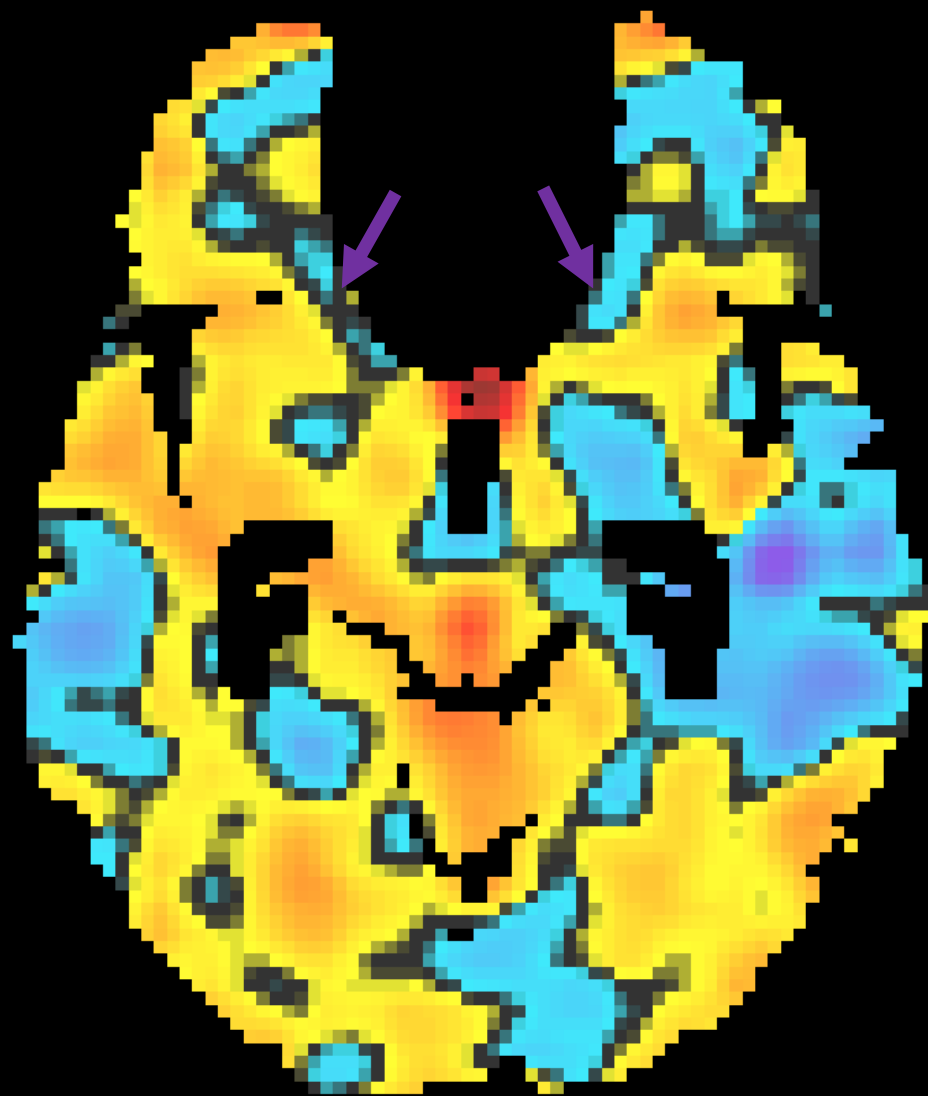
BOLD O<sub>2</sub> Ramp



t-scores



Hyperoxia – BL pCASL



Flow

80

60

40

20

0

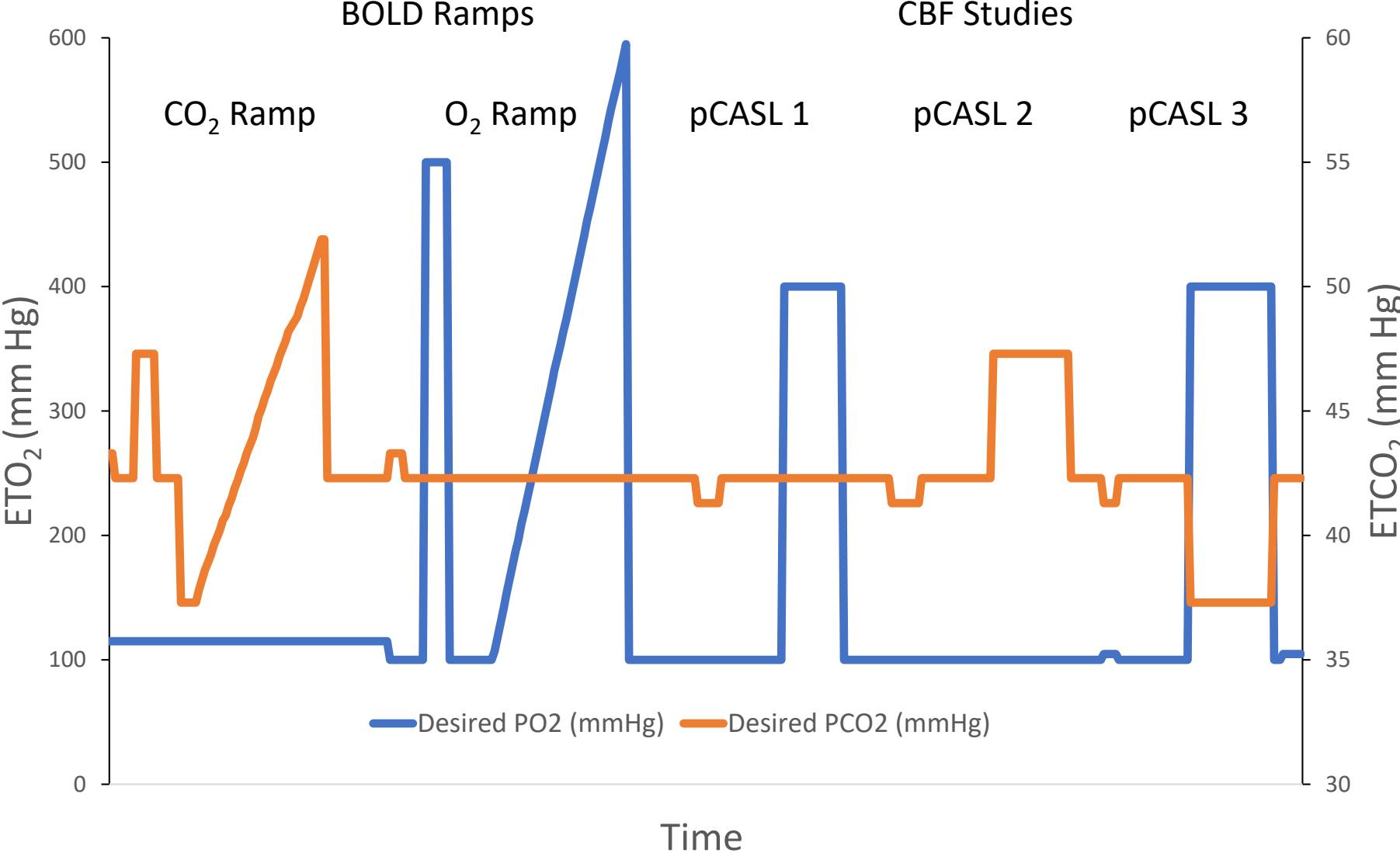
-20

-40

-60

-80

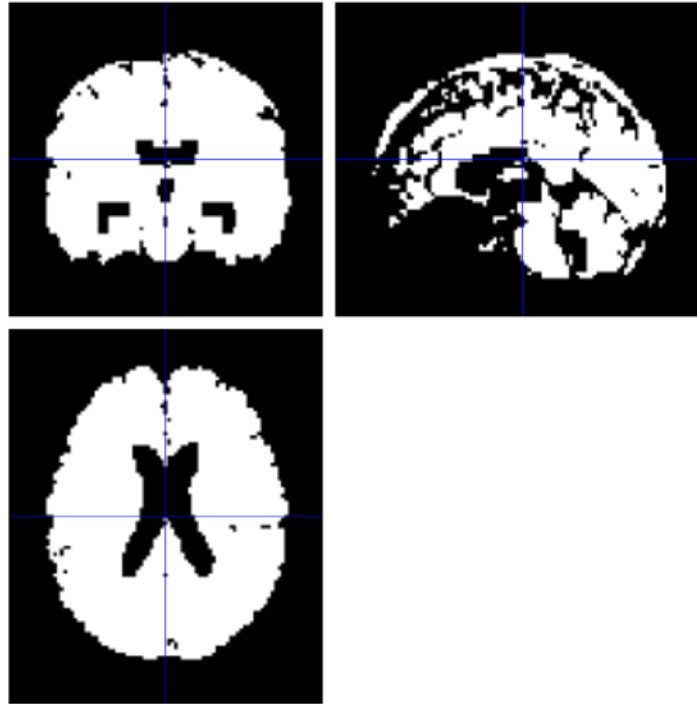
# ET Gas Protocol



## Supplemental File 2

Images were acquired using a Siemens Verio 3.0 T MR scanner with a 12-channel phased-array head coil. Anatomical imaging was acquired without manipulation of end-tidal gases using a sagittal 3D T1 MPRAGE (whole brain coverage; matrix:  $256 \times 256$ ; slice thickness: 2.2 mm; no interslice gap; voxel size  $2 \text{ mm} \times 2 \text{ mm} \times 2 \text{ mm}$ ) and axial gradient recalled echo planar (GRE) sequences to screen for cerebral microhemorrhages as well as GRE B0-field mapping. CVR was assessed using continuous BOLD MRI during MPET CO<sub>2</sub> targeting. BOLD MRI data were acquired using a T2\*-weighted single-shot gradient echo pulse sequence with echoplanar readout (field of view:  $24 \text{ cm} \times 24 \text{ cm}$ ; matrix:  $64 \times 64$ ; TR: 2,000 ms; TE: 30 ms; flip angle: 85°; slice thickness: 5.0 mm; interslice gap: 2.0 mm; voxel size  $3.75 \times 3.75 \times 6 \text{ mm}$ ; number of temporal frames = 330; 10 s of initial imaging data was discarded to allow for equilibration). Global mean resting CBF was assessed using pseudo-continuous arterial spin labeling (pCASL) that included an initial M0 scan—Siemens ep2d\_pCASL—echo planar readout (field of view  $24 \text{ cm} \times 24 \text{ cm}$ , TR 8,000 ms, TE 12 ms, contrast with a flip angle 90°, 20 slices, CASL method—multislice, label offset 90 mm, post label delay 1,200 ms, crusher gradient 0 s/mm<sup>2</sup>, and voxel size  $3.8 \text{ mm} \times 3.8 \text{ mm} \times 5.0 \text{ mm}$ ). The formal pCASL sequence then followed consisting of an echo planar readout (field of view  $24 \text{ cm} \times 24 \text{ cm}$ , TR 4,000 ms, TE 12 ms, contrast with a flip angle 90°, 20 slices, slice thickness 5.0 mm, CASL method—multislice, label offset 90 mm, post label delay 1,200 ms, crusher gradient 0 s/mm<sup>2</sup>; voxel size  $3.8 \text{ mm} \times 3.8 \text{ mm} \times 5.0 \text{ mm}$ ). Imaging duration was for 3 min. The first two labeled–non-labeled pairs were discarded.

# Supplemental File 3: B0 heterogeneity correction



Crosshair Position

mm:

vc:

Intensity:

right (mm)	<input type="text" value="0"/>
forward (mm)	<input type="text" value="0"/>
up (mm)	<input type="text" value="0"/>
pitch (rad)	<input type="text" value="0"/>
roll (rad)	<input type="text" value="0"/>
yaw (rad)	<input type="text" value="0"/>
resize {x}	<input type="text" value="1"/>
resize {y}	<input type="text" value="1"/>
resize {z}	<input type="text" value="1"/>

Reorient images...

File: `..lmask_gm+wm-B0+Ventr.img`

Dimensions: 91 x 109 x 91

Datatype: int16

Intensity: Y = 3.05185e-05 X

**spm - algebra**

Vox size: -2 x 2 x 2

Origin: 46 64 37

Dir Cos: 1.000 0.000 0.000  
0.000 1.000 0.000  
0.000 0.000 1.000

Full Volume	<input type="button" value="Hide Crosshairs"/>
World Space	<input type="button" value="bilin interp"/>
Auto Window	<input type="button" value="Add Blobs"/>

# 2<sup>nd</sup> Level Group Comparison CO<sub>2</sub> and O<sub>2</sub> Inverse Responses

